

# THE MARK II SILICON STRIP VERTEX DETECTOR AND PERFORMANCE OF A SILICON DETECTOR TELESCOPE IN THE MARK II DETECTOR AT THE SLC\*

LUIS LABARGA, CHRIS ADOLPHSEN, GIORGIO GRATTA,  
ALAN LITKE, MICHAL TURALA AND CARLA ZACCARDELLI

*Santa Cruz Institute for Particle Physics  
University of California, Santa Cruz, CA 95064*

ALAN BREAKSTONE AND SHERWOOD PARKER

*University of Hawaii, Honolulu, HI 96822*

BRUCE BARNETT, PAUL DAUNCEY, DAVID DREWER AND JOHN MATTHEWS

*Johns Hopkins University, Baltimore, MD 21218*

ROBERT JACOBSEN AND VERA LÜTH

*Stanford Linear Accelerator Center  
Stanford University, Stanford, California 94309*

## Abstract

A Silicon Strip Vertex Detector (SSVD) consisting of 36 independent silicon detector modules has been built for use in the Mark II detector at the SLAC Linear Collider (SLC). We discuss the performance of the individual modules and the stability and accuracy of their placement in the mechanical support. To gain operational experience at the SLC, we have assembled and placed inside the Mark II a telescope made of three Silicon Detector Modules. We present results from the first data run of the SLC on the overall performance of the Telescope, including backgrounds, charged particle tracking and spatial resolution.

## I. INTRODUCTION

To enhance the study of short lived particles produced in  $Z^0$  decays, we have built a silicon strip vertex detector (SSVD) for the Mark II experiment at the SLAC Linear Collider (SLC).

The SSVD is expected to be among the first high resolution silicon vertex detector operating in a colliding beam

\* Work supported by Department of Energy, Contracts DE-AM03-76SF00010, DE-AC03-89ER40103, and DE-AC03-76SF00515, and the National Science Foundation (John Hopkins).

experiment. An important feature of this device is the VLSI read-out. As we have described in previous publications<sup>[1][2]</sup>, the SSVD consists of three co-axial layers of silicon strip detector modules (SDM's) located outside the beam pipe at radii of 29 mm, 33 mm and 37 mm (Figure 1).

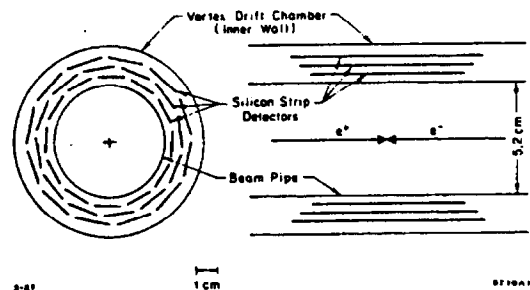


Figure 1. The Layout of the Silicon Strip Vertex Detector.

There are twelve SDM per layer. Their main component is a 300  $\mu\text{m}$  thick silicon detector. Each silicon detector has 512 strips that run parallel to the beam direction and are wire-bonded to four custom VLSI chips (Microplex<sup>[3]</sup>). The Microplex chips are epoxied onto a hybrid circuit which provides the control lines, a switchable capacitor bank for the power, and a differential amplifier and line driver for the analog output (Figure 2).

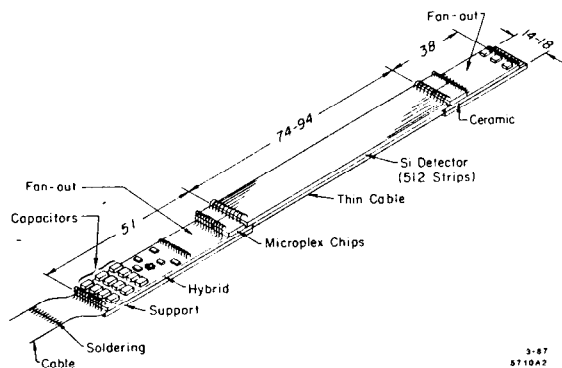


Figure 2. The plan for a silicon detector module.

The modules are housed in two half cylindrical structures. Each consists of two slotted aluminum endplates that are joined by inner and outer 250  $\mu\text{m}$  thick beryllium shells. Spring loaded fixtures are attached to the two ends of the modules and hold them in the endplate slots. The two halves of the structure are each attached to the central section of the vacuum pipe by a three-point mount.

The expected impact parameter resolution  $\sigma_b$  for the SSVD can be approximated as<sup>[1]</sup>  $\sigma_b = \sqrt{5^2 + (37/p)^2}$  where  $\sigma_b$  is in  $\mu\text{m}$  and  $p$  is the track momentum in  $\text{GeV}/c$ . The hits from the Vertex Drift Chamber (VDC) and Central Drift Chamber (CDC)<sup>[4]</sup> have been included in the tracking used to derive the above result. The first term comes from the intrinsic resolution of the silicon detector (as measured in a test beam experiment<sup>[5]</sup>) and the second term is the multiple scattering contribution.

Presently the SSVD is installed in the Mark II detector at the SLC interaction point (IP). Data taking is scheduled to start in January 1990.

## II. PERFORMANCE OF SILICON DETECTOR MODULES

We have assembled and tested more than 40 SDM's. To estimate signal-to-noise ratios and gains of individual strips we have measured signals from 60  $\text{keV}$  X-rays emitted by a  $^{241}\text{Am}$  source. For comparison, the most probable energy loss of minimum ionizing particles in our detectors at normal incidence is 85  $\text{keV}$ . We define the signal-to-noise ratio ( $S/\sigma_{\text{noise}}$ ) as the total signal height divided by the r.m.s. noise on a single strip. The distribution of the average  $S/\sigma_{\text{noise}}$  per module is shown in Figure 3. It has a mean value of 12.6 corresponding to 17.6 for the most

probable value of energy loss for a minimum ionizing particle at normal incidence. In Figure 3 the signal has been scaled to that of a minimum ionizing particle.

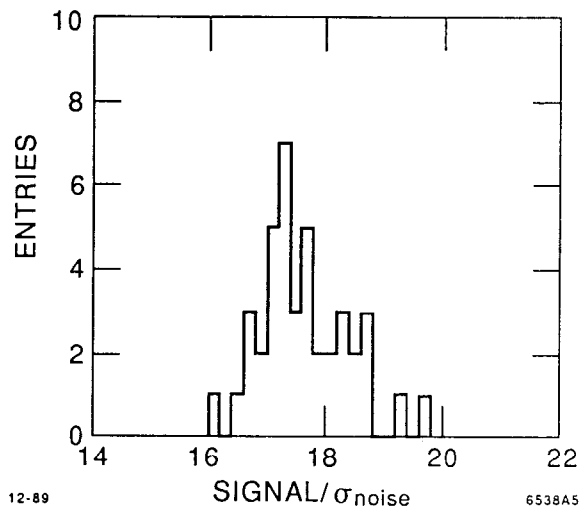


Figure 3. Average signal-to-noise ratio for each module. The signal is scaled to that of a minimum ionizing particle.

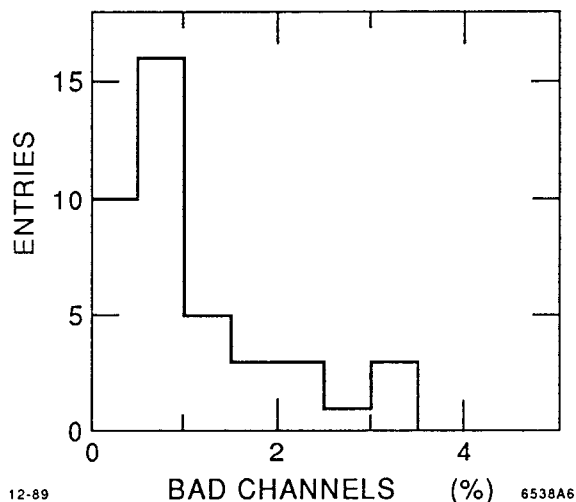


Figure 4. Bad channels distribution for each SDM of the production.

All the routine testing of the modules during and after the assembly was done by sending calibration pulses to the input lines of the Microplex chips. The amplitude of those pulses were set in such a way as to give a calibration signal-to-noise ratio ( $R_c$ ) roughly equal to the one expected for minimum ionizing particles at normal incidence. Although this technique is not precise enough to measure the gain of each channel to the accuracy required for track reconstruction, it is good enough to allow a bad channel characterization. If we define as bad a channel

with  $R_c/\bar{R}_c < 0.5$  or  $R_c/\bar{R}_c > 2$ , where  $\bar{R}_c$  is the average on each module, we obtain the distribution of the number of bad channels per module shown in Figure 4. The total fraction of bad channels for all SDM's is 1.1 %. The main cause is large leakage currents in the silicon detector.

### III. ACCURACY AND STABILITY OF THE PLACEMENT OF THE SDM'S IN THE MECHANICAL SUPPORT

The excellent intrinsic spatial resolution of the SSVD modules of  $5 \mu\text{m}$  places stringent demands on the precision, alignment and rigidity of the support structure. In particular, the strips have to be placed to within  $1 \text{ mrad}$  parallel to the symmetry axis so that the 1-2 mm uncertainty in the extrapolated CDC track position along this axis will not contribute significantly to the error in the coordinate measurement by the SSVD.

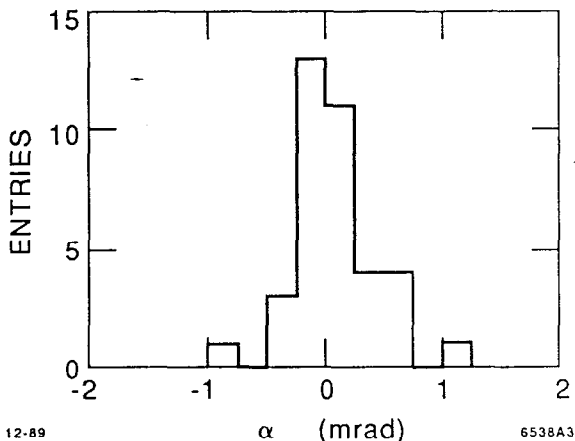


Figure 5. Parallelism angle ( $\alpha$ ) between the strips and the holder axis.

The slotted aluminium endplates were cut in pairs by electro-discharge machining so as to obtain accurate relative position of the slots in the two ends. We have verified that the dimensions and locations of the slots are accurate to  $15 \mu\text{m}$ . The spring fixtures limit the relative movements of the two ends to less than  $1\text{-}2 \mu\text{m}$ . The individual modules were loaded with the holder mounted on a rotation stage, layer by layer. The placement and exact shape of the detector surfaces were measured with an optical microscope of high precision:  $1 \mu\text{m}$  horizontal and  $2 \mu\text{m}$  vertical. Figure 5 shows the measured parallelism angle ( $\alpha$ ) between the strips and the holder axis for the 36 SDM's

in their final position in the SSVD holder. Overall, angles are within tolerances.

Once a detector half was fully loaded and closed with the outer beryllium shell, the relative positions of the modules were remeasured using a collimated X-ray beam as described in a recent paper.<sup>[6]</sup> As a check of the stability of the measurements they were redone after two months time. In that interval the detector half was remounted on the dummy beam pipe in an attempt to simulate the transport and installation procedure. Figure 6 shows a histogram of the differences in the measurement of the position of the centers of the detectors after allowing for a global transformation of the half cylinder between measurements. Our goal was a stability of  $< 2\text{-}3 \mu\text{m}$ . All but two modules are within tolerance. A possible explanation for those two is that there was some slippage of their respective cables in the cable clamp structure used to isolate cable motion from the modules.

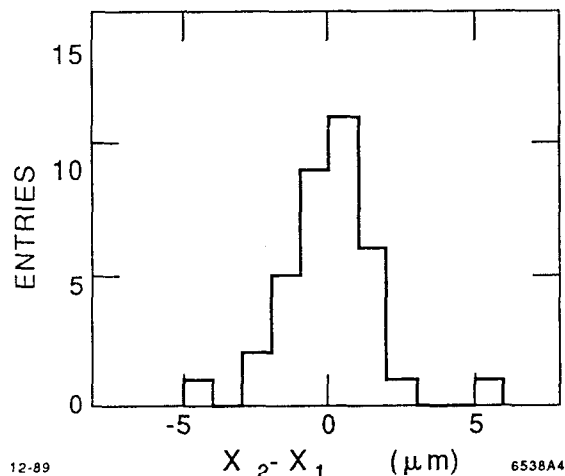


Figure 6. Difference between two sets of X-rays measurements of the positions of the centers of the detector modules.

### IV. THE SILICON DETECTOR TELESCOPE

To gain operational experience at the SLC, we have assembled and placed inside the Mark II a telescope made of three Silicon Detector Modules.

The Telescope has been placed on the current SLC beam pipe such that the modules are at radii of 43 mm, 48 mm and 53 mm from the SLC IP. The housing and mechanical stability is provided by a rectangular box made of 3.3 mm thick lucite (bottom and sides) and 0.9 mm thick aluminum

(top cover). The relative alignment of the modules was measured using the X-ray set-up. The strips are parallel within 0.5 mr. The parallelism between the Telescope and the Mark II  $z$  axis is of the order of 5 mr. Figure 7 shows the Telescope layout and its location at the Mark II/SLC beam pipe. The solid angle from the IP covered by the region of overlap of at least two modules is 1.3 % of the total  $4\pi$  sr.

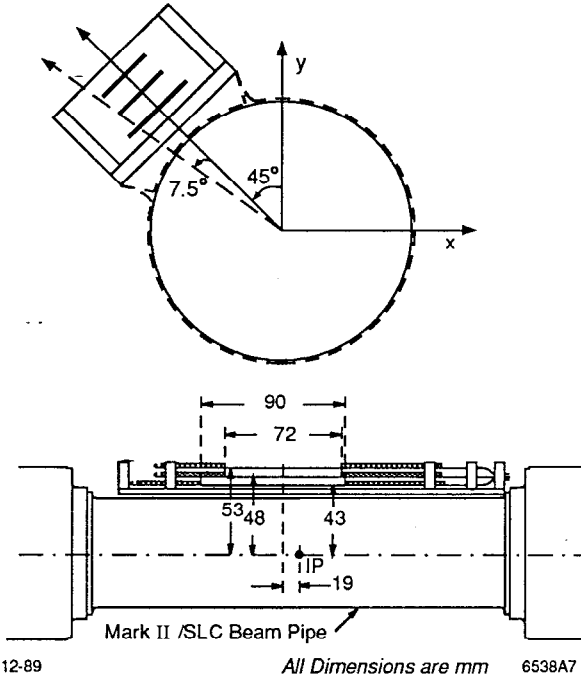


Figure 7. Layout of the Silicon Telescope and its location on the Mark II/SLC beam pipe.

The 3 x 512 output signals from the Telescope are multiplexed to a single modified BADC CAMAC module<sup>[7]</sup> which performs analog-to-digital conversion, pedestal subtraction and event-by-event baseline shift and channel gain corrections. The BADC searches the data for clusters defined as three contiguous strips with a total pulse height above the sum of the thresholds stored for these channels. The threshold for each strip is taken to be  $1.5\sigma_{noise}$ , where  $\sigma_{noise}$  is the r.m.s. noise as measured by the width of the pedestal distribution. When a cluster is found, those channels plus one on each side are stored for later transfer to the Mark II VAX. A Telescope event display is shown in Figure 8 for one of the  $Z^0$  decays recorded by the Mark II. Five clear tracks can be seen (the dashed lines are to guide the eye). The two uncorrelated clusters in the bottom module are believed to be two other particles which

passed outside the area covered by the middle and top modules.

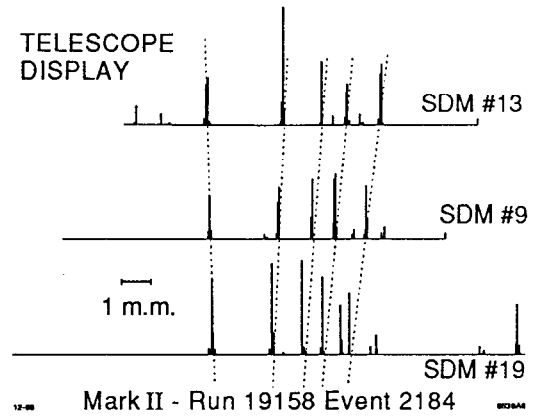


Figure 8. Telescope event display for one  $Z^0$  decay. The dashed lines are to guide the eye.

The modules in the telescope were rejects from the SDM production. About 7% of the channels are considered as bad as defined in section II. The main reasons are large leakage currents in some areas of the detectors, open wire bonds, and shorts between wire bonds. These channels and their immediate neighbors have been excluded from the analysis.

Data taking started in March 1989 and continued until the first week of September. For this analysis we have only used tracks coming from  $Z^0$  decays. The total number of  $Z^0$ 's produced by the SLC during that period is 350. From their decay, we estimate at least 100 tracks crossed at least two of the Telescope's silicon detectors.

#### A. Occupancies

We have used the Telescope to study the occupancies expected in normal operation due to accelerator related background. Note that the Telescope's inner most module is at about the same radial distance to the IP as the SSVD outermost layer of modules. We have used randomly triggered events distributed uniformly over the running period. If we define the occupancy in the Telescope as the ratio between the number of read-out strips with a pulse height larger than  $1.5\sigma_{noise}$  and the total number of good strips, we get  $0.6 \pm 0.2\%$ . For the sake of comparison, the drift chamber occupancy (defined as the ratio between the number of wires fired and the total number of wires) was  $7 \pm 0.2\%$ .

### B. Telescope - Central Drift Chamber track matching

The offline analysis starts by looking for clusters as follows<sup>[5]</sup>: (1) we search for a strip with pulse height above  $4.5\sigma_{noise}$  to begin the cluster; (2) we add any immediately adjacent strips with pulse height above  $1.5\sigma_{noise}$ ; and (3) we repeat step 2 until the adjacent strip pulse heights fall below the cut. The spatial position of a cluster is then calculated by taking the pulse-height-weighted average coordinate of all the strips included in the cluster. To avoid large Landau fluctuations and background contamination we have used only reconstructed clusters with a pulse height smaller than  $36\sigma_{noise}$ .

To correct the cluster positions for the internal alignment of the modules we need to know the  $z$  position of the cluster. Because the  $z$  information is provided by the CDC only, we need to know to which CDC track corresponds a given Telescope track. We start by establishing candidate Telescope tracks: (a) sets of three clusters pointing to the IP within 20 mm such that the reconstructed position in the middle Telescope module minus the expected value from the straight line formed with the positions in the inner and outer modules (we will call the quantity  $\Delta$ ) is smaller than  $100 \mu m$  and (b) sets of two clusters pointing to the IP within 20 mm.

We next associate a candidate Telescope track to the CDC track which minimizes the differences in their positions and angles. Only those CDC tracks with momentum  $p > 0.250$  GeV have been considered. A  $\chi^2$  algorithm has been used. Candidate tracks were rejected if the  $\chi^2$  for the best matching was above a quality cut. One should note that the alignment of the Telescope as a whole with respect to the Mark II detector was done iteratively to minimize the resulting  $\chi^2$  distribution of the matched tracks.

Figure 9 shows the distributions after matching for  $\frac{\delta x}{\sigma_{\delta x}} = \frac{X_{CDC} - X_{TEEL}}{\sigma_{\delta x}}$  (a) and  $\frac{\delta \phi}{\sigma_{\delta \phi}} = \frac{\phi_{CDC} - \phi_{TEEL}}{\sigma_{\delta \phi}}$  (b) where  $\phi$  is the azimuthal angle and  $X$  is measured in the  $r\Phi$  direction along the outer module.  $\sigma_{\delta x, \phi}$  are the expected measurement errors. The widths of the distributions are  $1.4 \pm 0.1$  and  $1.3 \pm 0.1$  respectively. They approach the expected value of unity when demanding isolation or high quality in the reconstruction of the CDC track.

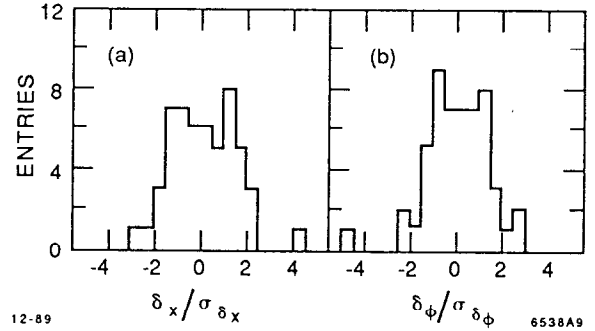


Figure 9. Distributions for  $\frac{\delta x}{\sigma_{\delta x}} = \frac{X_{CDC} - X_{TEEL}}{\sigma_{\delta x}}$  (a) and  $\frac{\delta \phi}{\sigma_{\delta \phi}} = \frac{\phi_{CDC} - \phi_{TEEL}}{\sigma_{\delta \phi}}$  (b), obtained after the CDC-Telescope track matching.

From a visual scan of all the events we estimate: i) 2 % of the matches were wrong. ii) 20 % of the obvious matches were not achieved because of large  $\chi^2$ . Those tracks are in dense jet environments. This fact and the improvement of the matching distributions with the quality and isolation of the CDC track discussed above, suggest that the track parameter measurement by the CDC is degraded in dense jets. The matching is expected to improve significantly with the inclusion of the VDC in the tracking system.

### C. Spatial resolution

To study the internal resolution of the Telescope we use the quantity  $\Delta$  defined in the previous section for all the three-cluster tracks with  $p > 1$  GeV. After correcting the cluster positions with the internal alignment constants we obtain the distribution shown in Figure 10. There is an event far away in the left tail which will be discussed later. Ignoring that event, the  $\Delta$  distribution is centered at  $\bar{\Delta} = -1.9 \pm 1.0 \mu m$  with a width  $\sigma_{\Delta} = 5.1 \pm 0.7 \mu m$ .

From  $\sigma_{\Delta}$  we can derive the spatial resolution of the silicon modules  $\sigma_{x_M}$ . Assuming  $\sigma_{x_M}$  to be the same for the three modules, we obtain  $\sigma_{x_M} = \sqrt{\frac{2}{3}}\sigma_{\Delta} = 4.2 \pm 0.6 \mu m$ . The multiple scattering contribution to  $\sigma_{x_M}$  is estimated to be of the order of the statistical error. Notice that the data have been taken over a time interval of six months. A comparison of the above resolution with our beam tests results indicates that the internal module alignment stayed stable at the micron level.

A likely explanation for the track with large  $\Delta$  is that a background hit occurred very near to the "true" track cluster. This is consistent with the broader width that we observe for this cluster. From the measured occupancy (see

section 4.A),  $\bar{w}\bar{e}$  estimate a  $\approx 35\%$  probability for one of the strips of the clusters in the sample (or one of the adjacent strips) to have extra pulse height due to background.

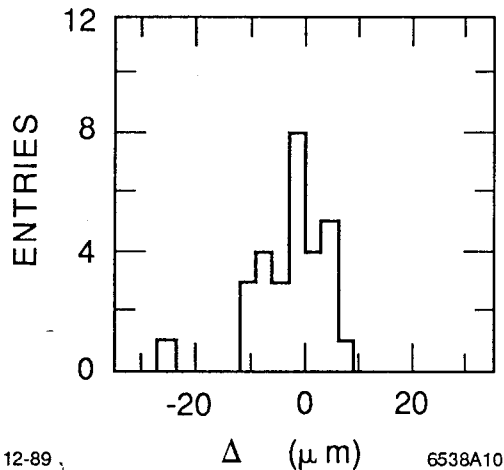


Figure 10.  $\Delta$  distribution as measured by the Silicon Telescope.

## V. SUMMARY

A Silicon Strip Vertex Detector (SSVD) consisting of 36 independent silicon detector modules has been built for use in the Mark II detector at the SLAC Linear Collider (SLC). The measured signal-to-noise ratio is typically 17.6 and the total fraction of bad channels is 1.3%. We have studied the stability and accuracy of the placement of the modules in the mechanical support. The strips are parallel to the holder axis to within 1 *mr*. The stability of the modules is typically better than 2-3  $\mu\text{m}$ .

To gain operational experience at the SLC, we have assembled and placed inside the Mark II a telescope made of three SDM's. Strip occupancies are less than 1%. Charged particle tracking has been studied with the decay products of  $Z^0$ 's. We obtain a position resolution of  $\sigma_{X_M} = 4.2 \pm 0.6 \mu\text{m}$ .

### Acknowledgements

We warmly acknowledge Vladimir Golubev (Nobosibirsk) and Michel Lateur (SLAC) for their help with data analysis and design respectively.

## REFERENCES

1. A. Litke et al.; Nucl. Instrum. & Methods A265 (1988) 93.
2. C. Adolphsen et al.; IEEE Trans. Nucl. Sci. NS-35 (1988) 424.
3. J. T. Walker et al.; Nucl. Instrum. & Methods 226 (1984) 200.
4. Mark II Coll., G. S. Abrams et al.; Nucl. Instrum. & Methods A281 (1989) 55.
5. C. Adolphsen et al.; Nucl. Instrum. & Methods A253 (1987) 444.
6. C. Adolphsen et al.; SLAC-PUB-4961, Apr. 1989; Presented at European Symp. on Semiconductor Detectors, Munich, Feb. 1989.
7. M. Breidenbach et al.; IEEE Trans. Nucl. Sci. NS-25 (1978) 706.